Journal of Theoretical Biology 383 (2015) 116–129

Contents lists available at ScienceDirect

Journal of Theoretical Biology

journal homepage: www.elsevier.com/locate/yjtbi

The evolutionary advantage of haploid versus diploid microbes in nutrient-poor environments

Kazuhiro Bessho [a,*], Yoh Iwasa [b], Troy Day [c]

[a] Department of Zoology, The University of British Columbia, Vancouver, BC V6T 1Z4, Canada
[b] Department of Biology, Faculty of Sciences, Kyushu University, Fukuoka 812-8581, Japan
[c] Department of Mathematics and Statistics, Queen's University, Kingston, ON K7L 3N6, Canada

HIGHLIGHTS

- We studied the relative advantages of haploidy versus diploidy in microbes.
- We examined the nutrient-limitation hypothesis theoretically.
- Energy conversion efficiency and scaling of mortality with cell size are key.
- We compared our theoretical predictions with empirical observations.

ARTICLE INFO

Article history:
Received 21 October 2014
Received in revised form
18 July 2015
Accepted 21 July 2015
Available online 4 August 2015

Keywords:
Ploidy evolution
Microbe life history model
Population dynamics
Allometry
Mathematical model

ABSTRACT

Sexual eukaryotic organisms are characterized by haploid and diploid nuclear phases. In many organisms, growth and development occur in both haploid and diploid phases, and the relative length of these phases exhibits considerable diversity. A number of hypotheses have been put forward to explain the maintenance of this diversity of life cycles and the advantage of being haploid versus that of being diploid. The nutrient-limitation hypothesis postulates that haploid cells, because they are small and thus have a higher surface area to volume ratio, are advantageous in nutrient-poor environments. In this paper, we examine this hypothesis theoretically and determine the conditions under which it holds. On the basis of our analysis, we make the following predictions. First, the relative advantages of different ploidy levels strongly depend on the ploidy-dependent energy conversion efficiency and the scaling of mortality with cell size. Specifically, haploids enjoy a higher intrinsic population growth rate than diploids do under nutrient-poor conditions, but under nutrient-rich conditions the intrinsic population growth rate of diploids is higher, provided that the energy conversion efficiency of diploids is higher than that of haploids and the scaling of mortality with cell size is weak. Second, differences in nutrient concentration in the inflowing medium have almost no effect on the relative advantage of ploidy levels at population equilibrium. Our study illustrates the importance of explicit modeling of microbial life history and population dynamics to understand the evolution of ploidy levels.

1. Introduction

Sexual eukaryotic organisms are characterized by haploid and diploid nuclear phases (Mable and Otto, 1998). The diploid phase is dominant among most advanced taxa with complex body structures, and many hypotheses have been advanced to explain the evolution of a prolonged diploid phase (Coelho et al., 2007; Crow and Kimura, 1965; Kondrashov and Crow, 1991; Lewis and Wolpert, 1979; Perrot et al., 1991). However, hypotheses that predict that only diploidy has an adaptive benefit do not satisfactorily explain the evolutionary persistence of haploidy and haploid–diploid life cycles (Hughes and Otto, 1999; Mable and Otto, 1998).

In many organisms, growth and development occur in both haploid and diploid phases, and the relative length of these phases displays considerable diversity (Bell, 1994; Mable and Otto, 1998). For example, eukaryotic algae show various patterns of alternating generations. Especially notable is the diversity of heteromorphic life cycles, in which distinct haploid and diploid generations alternate (Abbott and Hollenberg, 1993; Bell, 1997; Bessho and Iwasa, 2010; Dring, 1992; Van den Hoek et al., 1995). In some species with a heteromorphic life cycle (e.g., family *Laminariaceae*, *Palmaria palmata*, *Kornmannia leptoderma*), the diploid phase develops into large-sized multicellular algal body but the haploid

* Corresponding author. Tel.: +1 604 8222131; fax: +1 604 822 2416.
E-mail addresses: bessho@zoology.ubc.ca (K. Bessho), yohiwasa@kyudai.jp (Y. Iwasa), tday@mast.queensu.ca (T. Day).

http://dx.doi.org/10.1016/j.jtbi.2015.07.029
0022-5193/

phase is microscopic, whereas in others (e.g., genus *Scytosiphon*, family *Bangiaceae*, genus *Monostroma*) the opposite is true (Bell, 1994; Dring, 1992; Hori, 1994).

These life cycle differences are observed in all three major divisions of macroalgae (Chlorophyta, Phaeophyta, and Rhodophyta) across many different lineages (Bell, 1994; Dring, 1992; Hori, 1994), which indicates that the relative dominance of the ploidal phases in algal life cycles is evolutionarily labile. Thus, theoretical studies have focused mainly on the evolutionary mechanisms by which these diverse life cycles are maintained and the trade-offs between being haploid versus being diploid (Coelho et al., 2007; Jenkins, 1993; Lewis, 1985; Nuismer and Otto, 2004; Orr and Otto, 1994; Otto and Marks, 1996).

Various developmental, genetic, and ecophysiological hypotheses have been put forward to explain the maintenance of such diverse life cycles. Developmental hypotheses posit that the diploid cell is essential for the development of complex structures (Bell, 1994; Perrot, 1994), whereas genetic hypotheses focus on the genetic advantages. For example, diploids can repair DNA damage by using the remaining intact chromosome as a template (Michod and Gayley, 1994), mask recessive deleterious mutations (Gerstein and Otto, 2009; Kondrashov and Crow, 1991; Mable and Otto, 2001; Otto and Goldstein, 1992; Otto and Marks, 1996; Perrot et al., 1991), evolve more rapidly (Lewis and Wolpert, 1979; Orr and Otto, 1994), and harbor a greater diversity of recognition molecules to help prevent infection by parasites (M'Gonigle and Otto, 2011; Nuismer and Otto, 2004).

Ecophysiological hypotheses focus on how ploidy affects an organism's adaptation to its environment (Cavalier-Smith, 1978; Lewis, 1985). A positive correlation between nuclear DNA content and cell volume has been reported in angiosperm plants (Bennett, 1972; Martin, 1966; Price et al., 1973), vertebrate animals (Commoner, 1964; Olmo and Morescalchi, 1978; Pagel and Johnstone, 1992), prokaryotic bacteria (Commoner, 1964), and algae (Holm-Hansen, 1969). This correlation is observed across ploidy levels and regardless of the number of nuclei in a cell or the cell size in angiosperms (Jovtchev et al., 2006; Melaragno et al., 1993), yeast (Galitski et al., 1999), and algae (Goff and Coleman, 1990). A strong correlation between the DNA content and the cell cycle length has also been reported (Bennett, 1971; Van't Hof, 1965; Van't Hof and Sparrow, 1963). These observations led Cavalier-Smith (1978) to suggest that the evolution of ploidy levels is a by-product of selection for cell size: conditions favoring small individuals with rapid growth rates select for haploidy, whereas conditions favoring large individuals select for diploidy. This is known as the Cavalier-Smith hypothesis.

Lewis (1985) has pointed out that the Cavalier-Smith hypothesis is insufficient because it does not explain the successional patterns of unicellular marine algae. Under the classical r- and K-selection hypothesis for a freshwater environment, small algae with higher population growth rates should appear early and large taxa occur toward the end of the succession when nutrients are limited. However the generally acknowledged successional pattern in marine environments is one where unicellular diploid diatoms tend to dominate early in a sequence of succession (Lewis 1985). To overcome the shortcomings of the Cavalier-Smith hypothesis, Lewis proposed a nutrient-sparing hypothesis (or nutrient-scarcity hypothesis), which explains the evolution of haploid organisms in relation to the energy supply. He suggested that haploidy might be more advantageous than diploidy under nutrient-limited conditions because haploid organisms have lower DNA replication costs.

The combination of these two hypotheses is known as the nutrient-limitation hypothesis (or nutrient-saving hypothesis). According to this hypothesis, diploids, which are simply double haploids, grow as fast as, or possibly faster than, haploids in nutrient-rich environments: although having twice as much DNA means that mRNA transcription can occur twice as fast, the speed advantage is canceled out by the larger cell volume. Therefore, the nutrient utilization efficiency of diploids is almost the same as that of haploids. In contrast, haploid cells enjoy an advantage in nutrient-poor environments, because the smaller haploid cells are better able to deal with nutrient scarcity owing to their greater ratio of surface area to volume (Coelho et al., 2007; Mable and Otto, 1998; Otto and Gerstein, 2008; Perrot, 1994).

The nutrient-limitation hypothesis has been tested by competition experiments performed with unicellular yeasts in chemostats and by measurement of body growth rates in multicellular juvenile red macroalgae raised under different nutrient conditions. The results of these experiments are not conclusive, however. For example, Adams and Hansche (1974) reported no significant difference in the maximum population growth rate between haploid and diploid yeasts in nutrient-rich chemostats, but they also found that haploid cells grew more rapidly than diploid cells when growth was limited by organic phosphate availability. Similarly, Glazunov et al. (1989) reported that diploid yeasts displaced haploid yeasts in rich media, although they also found that haploid cells had an advantage over diploid cells in minimal media, and in the presence of a competitor (the yeast *Pichia pinus*). However, Naĭdhardt and Glazunov (1991) reported that diploids completely displaced haploids in both rich and minimal media, and diploids also have an advantage over haploids in the presence of a competitor. Similarly in an experiment comparing growth rates between isomorphic haploid and diploid phases in the juvenile red alga *Gracilaria verrucosa*, Destombe et al. (1993) found that the haploid stage had a growth advantage under nutrient-poor conditions and diploids had an advantage in nutrient-rich seawater. In the isomorphic red alga *Polcavernosa debilis*, however, Littler et al. (1987) reported no significant differences in net photosynthesis or calorific content across ploidy levels.

In this paper, we develop life history models of unicellular microbes with ploidy-dependent parameters to help us to understand these experimental outcomes.

2. Model

To determine the effect of nutrients on the relative advantage of haploid versus diploid phases, we developed two models of a unicellular microbe with asexual reproduction. The first model, which is the simplest, assumes that nutrient levels are fixed and populations of microbes grow exponentially. In this density-independent model, we evaluate the relative advantage of the two ploidy levels by comparing their intrinsic population growth rates. In the second model, we incorporate density-dependence in the population dynamics and quantify the relative advantage of the different ploidy levels by determining under what circumstances one outcompetes the other. Parameters and variables in our model are listed in Table 1.

2.1. Life history of unicellular microbes

Both models assume the same microbial life history. The microbes of both ploidy levels proliferate asexually (or vegetatively) by binary fission. A generation starts at the ontogenetic time $\tau=0$ and ends at $\tau=T_p$. Suffix p is ploidy dependent; when $p=h$, the generation is haploid, and when $p=d$, it is diploid.

Within the lifespan of a microbe, the cell volume V_p increases according to the following differential equation and initial condition:

$$\frac{dV_p}{d\tau}=e_pU_p(V_p,N), \quad \text{for } 0\le\tau\le T_p, \tag{1a}$$

$$V_p(0)=v_p, \tag{1b}$$

where U_p denotes the rate of nutrient uptake per individual; N is the nutrient level, and e_p is the energy conversion efficiency into cell structure, which is assumed to be constant.

Table 1
The variables and parameters in the model.

Symbol	Interpretation
α	Cell size exponent
β	Surface area to volume ratio exponent
γ	Defense efficiency exponent
s	Energy conversion efficiency level of diploids relative to haploids
r	Handling time efficiency level of diploids relative to haploids
v_p	Initial volume of a haploid cell ($p=h$) or a diploid cell ($p=h$)
k	Proportional constant for allometric relationship
G_p	Amount of nuclear content
e_p	Energy conversion efficiency into cell structure
$\hat{h}_p$	Handling time for nutrient uptake process
h_p	Handling time efficiency
σ	Efficiency of the expected number of nutrient captures per unit time
m_0	Coefficient of mortality risk
τ	Cell ontogenic time
V_p	Cell volume
U_p	Unitrient uptake rate per individual.
N	Nutrient level in the media
T_p	Time interval between birth to binary fission (doubling time)
L_p	Suprivorship of a cell from the binary fission of the parent cell
ϕ_p	Intrinsic rate of population increase
f_{in}	Rate of inflow of the nutrient
f_{decay}	Rate of nutrient decay
f_{out}	Dilution rate in a chemostat
N_0	Nutrient concentration in the inflowing medium
t	Time for population dynamics
H	Population density of haploids
D	Population density of diploids
$\tilde{U}_p$	Average nutrient uptake rate
$\tilde{N}$	Nutrient level derived by quasi-equilibrium approximation

The Cavalier-Smith hypothesis (Cavalier-Smith, 1978) is mainly concerned with the correlation between nuclear DNA content and cell size. It is well known that there is a strong positive correlation between log[nuclear DNA content] and log[cell volume] in prokaryotic and eukaryotic species (Gregory, 2001; Ycas et al., 1965). We therefore assume that the initial cell volume v_p is related to the nuclear content G_p, by the following allometric relationship:

$$v_p := kG_p^{\alpha}, \tag{2}$$

where the positive exponent α is often approximately one ($\alpha \approx 1$; Gregory, 2001; Price et al., 1973) and k is a positive parameter. But we note that some studies have reported other allometric exponent values (Gregory, 2001). To describe nutrient-limitation hypothesis we assume $\alpha=1$ as basic parameter, and we leave this parameter arbitrary.

The nutrient-limitation hypothesis supposes that the nutrient uptake rate is regulated by surface area in a nutrient-poor environment. To describe the functional response of resource use and represent nutrient limited growth of microorganisms, the Michaelis–Menten equation from enzyme kinetics theory is often assumed (Monod, 1950; Herbert et al., 1956; Real, 1977; Edwards et al., 2012). Especially because many previous experimental research comparing haploid and diploid growth assume this relationship to analyze data (Francis and Hansche, 1972; Adams and Hansche, 1974), the following mathematically equivalent equation (Aksnes and Egge, 1991; Gentleman et al., 2003) is assumed

$$U_p := \frac{\sigma {V_p}^{\beta} N}{1+\hat{h}_p \sigma {V_p}^{\beta} N}, \tag{3}$$

which is known as the type II functional response (Solomon, 1949) or the disc equation (Holling, 1959). Eq. (3) can be understood as the average of a Poisson process in which the expected number of nutrient particles captured per unit time is proportional to the availability (or concentration) of nutrient N and surface area ${V_p}^{\beta}$. For spherical cells, exponent β is generally assumed to be 2/3, based on the relationship between cell volume and surface area. σ is a parameter denoting the expected number of nutrient captures per unit area and time, and $\hat{h}_p$ is handling time in the foraging process. The nutrient-limitation hypothesis assumes that a diploid cell is equivalent to two haploid cells when nutrient availability is sufficiently high (Perrot, 1994). To represent this assumption, we assume that the handling time is inversely proportional to the cell volume: $\hat{h}_p := h_p/V_p$, where h_p is handling time efficiency. By substituting this definition of $\hat{h}_p$ into Eq. (3), we find that the nutrient uptake rate U_p is proportional to the surface area ${V_p}^{\beta}$ in nutrient-poor environment. The nutrient uptake rate is proportional to volume V_p when the nutrient level N saturates in a nutrient-rich environment, and growth of single diploid cell is twice that of haploids because the sizes of exponentially growing cells are always proportional to initial cell size without advantage of ploidy levels (we discuss the effects of the form of the nutrient uptake rate function in Appendix A).

Upon binary fission, a unicellular microbe distributes half of its contents to each of two daughter cells. Therefore, the lifespan (i.e., the doubling time) T_p is determined by the equation $V_p(T_p)=2V_p(0)$. Here, we assume that the availability of nutrient N is approximately constant during the lifespan of the microbe (i.e., on time scale τ).

Let $L_p(\tau)$ be the survivorship of a cell from the fission of the parent cell to age τ. We assume that the survivorship function satisfies the differential equation,

$$\frac{dL_p}{d\tau} = -m(V_p)L_p, \tag{4a}$$

$$L_p(0)=1, \tag{4b}$$

where $m(V_p)$ is the instantaneous mortality, which is assumed to be a function of body size V_p. For simplicity, we consider the case where instantaneous mortality depends on cell size according to a power function

$$m(V_p) := \frac{m_0}{{V_p}^{\gamma}}, \tag{5}$$

where mortality coefficient m_0 is a non-negative constant. We normally assume that parameter $\gamma>0$ because microbes can escape from predators by having a large body size or by producing defensive substances. Instantaneous mortality becomes independent of cell size when $\gamma=0$ in Eq. (5).

By using these equations describing microbial life history, we can calculate the per capita rate of population growth ϕ_p as follows (Appendix A):

$$\phi_p = \frac{e_p\sigma(1-\beta)(\ln 2)N}{\left(2^{1-\beta}-1\right)v_p^{1-\beta}+h_p\sigma(1-\beta)(\ln 2)N} \left(1-\frac{m_0 v_p^{1-\beta-\gamma}\left(2^{1-\beta-\gamma}-1\right)}{e_p\sigma(1-\beta-\gamma)(\ln 2)N}-\frac{m_0 h_p v_p^{-\gamma}(1-2^{-\gamma})}{e_p\gamma(\ln 2)}\right). \tag{6}$$

The parameters and variables V_p, U_p, v_p, and L_p may depend on ploidy, and they are therefore related to genome size G_p. We also allow for ploidal differences in the energy conversion efficiency e_p and the handling time efficiency h_p. The genome of diploid cells is twice the size of that of haploid cells; hence, we can denote the relationship between the two genome sizes as $G_d=2G_h$. Therefore from Eq. (2), the initial volumes of the haploid and diploid cells are related as follows:

$$v_d = 2^{\alpha} v_h. \tag{7}$$

Parameters e_p and h_p in Eq. (6) are determined by the regulation (i.e., the expression or repression) of autosomal genes, the amount and activity of enzymes, and the cost of DNA production from phosphorus in the cell. We denote the ploidy-dependent

relationship of e_p and h_p between haploids and diploids as follows:

$$e_d = se_h, \tag{8a}$$

$$h_d = h_h/r, \tag{8b}$$

where s and r are the efficiency levels of diploids relative to those of haploids ($s>0$ and $r>0$). The nutrient-limitation hypothesis assumes that each of these parameters is approximately one ($s=r\approx 1$), because twice as much gene regulation is canceled out by the doubled volume of the diploid cell (Perrot, 1994).

2.2. Relative values of intrinsic population growth rates

By substituting Eqs. (7), (8a), and (8b) into Eq. (6), we can derive the intrinsic population growth rates of haploids and diploids as follows:

$$\phi_h = \frac{C_1 N}{C_2 + h_h C_3 N}\left(1 - \frac{m_0 C_4}{N} - m_0 h_h C_5\right), \tag{9a}$$

$$\phi_d = \frac{sC_1 N}{2^{\alpha(1-\beta)} C_2 + h_h (1/r) C_3 N}\left(1 - \frac{m_0 2^{\alpha(1-\beta-\gamma)} C_4}{sN} - \frac{m_0 h_h 2^{-\alpha\gamma} C_5}{sr}\right), \tag{9b}$$

where C_1, C_2, C_3, C_4, and C_5 are positive constants when $\gamma>0$ (see Appendix A).

In the density-independent model, the fitness measure is the intrinsic population growth rate ϕ. When $\phi_h>\phi_d$, haploids grow faster than diploids, and vice versa. Under this assumption, we can analyze the relative advantage of each in nutrient-poor (small N) and nutrient-rich (large N) conditions.

2.3. Population dynamics

In this model, we assume that the nutrient availability N is fixed. This is a good assumption when the population size of the focal microbe remains much lower than the carrying capacity and the availability of nutrients is not affected by the existence of the microbe. However, as the population size of the microbe increases by binary fission, the availability of nutrients in the medium decreases if there is no external nutrient supply, which reduces the growth rate of the microbes. In accordance with the life history of the microbe described in Sections 2.1 and 2.2, we develop a population dynamics model in which the availability of nutrients changes with time t. To be specific, we have the following model:

$$\frac{dH}{dt} = \phi_h(N)H, \tag{10a}$$

$$\frac{dD}{dt} = \phi_d(N)D, \tag{10b}$$

$$\frac{dN}{dt} = N_0 f_{in} - N f_{decay} - \tilde{U}_h H - \tilde{U}_d D. \tag{10c}$$

Here, H and D are the population density of haploids and diploids, $N_0 f_{in}$ denotes the rate of inflow of nutrients, and f_{decay} is the nutrient decay rate. In Eq. (10c), we assume that the nutrient uptake rate is equal to the average rate of nutrient uptake $\tilde{U}_p := \int_0^{T_p} U_p L_p d\tau/T_p$. For simplicity, we here assume that the nutrient dynamics are faster than the population dynamics of the organisms; hence, the nutrient level is assumed to be the equilibrium level of Eq. (10c), whereas H and D have not reached the equilibrium given by Eqs. (10a) and (10b). Then the quasi-equilibrium state for the nutrient dynamics is calculated by

$$\left.\frac{dN}{dt}\right|_{N=\tilde{N}} = N_0 f_{in} - \tilde{N} f_{decay} - \tilde{U}_h\left(\tilde{N}\right)H - \tilde{U}_d\left(\tilde{N}\right)D = 0. \tag{11}$$

Eq. (11) has only one stable solution (i.e., there is just one positive equilibrium density $\tilde{N}$) when $N>0$ (Appendix A). By substituting $\tilde{N}$ into Eqs. (10a) and (10b), we obtain a dynamical system for the two variables $H(t)$ and $D(t)$ by a quasi-equilibrium approximation.

2.4. Chemostat model

In Section 2.3, we considered the population dynamics when there is an inflow of nutrients and population sizes are regulated by mortality. So that we could compare our model with the results of chemostat experiments (Adams and Hansche, 1974), we also analyzed the population dynamics in a chemostat-type system. In chemostats (e.g. Herbert et al., 1956; Monod, 1950), population growth is limited by the dilution of the flowing medium, instead of by mortality, such that $m_0\approx 0$ (Francis and Hansche, 1972). As a result, we have

$$\frac{dH}{dt} = \phi_h(N)H - f_{out}H, \tag{12a}$$

$$\frac{dD}{dt} = \phi_d(N)D - f_{out}D, \tag{12b}$$

$$\frac{dN}{dt} = N_0 f_{out} - N f_{out} - \tilde{U}_h H - \tilde{U}_d D. \tag{12c}$$

where $f_{out}H$ and $f_{out}D$ represent the loss of individuals by washout. We assume the quasi-equilibrium state of the nutrient and the nutrient level is the same as those described by Eq. (11) when $f_{out}=f_{in}=f_{decay}$.

3. Results

3.1. Relative advantages of each ploidy when handling time is negligible ($h_p=0$)

In this section, we consider the case of a density-independent population, where the fitness measure is the intrinsic rate of population growth ϕ_p. Fig. 1 illustrates the relative success of the different ploidy levels on the (γ, s) plane. Our result involve four parameters, the advantage of diploids in energy conversion efficiency over the haploids s, the exponent of cell size α, the surface area to volume ratio β, and the scaling of mortality with cell size γ. The equations $s=2^{\alpha(1-\beta)}$ and $s=2^{\alpha(1-\beta-\gamma)}$ specify the boundaries separating the regions where haploidy or diploidy are relatively advantageous (Appendix B). When $0<s<2^{\alpha(1-\beta-\gamma)}$, haploidy is always more advantageous than diploidy. When $2^{\alpha(1-\beta-\gamma)}<s<2^{\alpha(1-\beta)}$, diploidy is more advantageous than haploidy in nutrient-poor environments, but the opposite

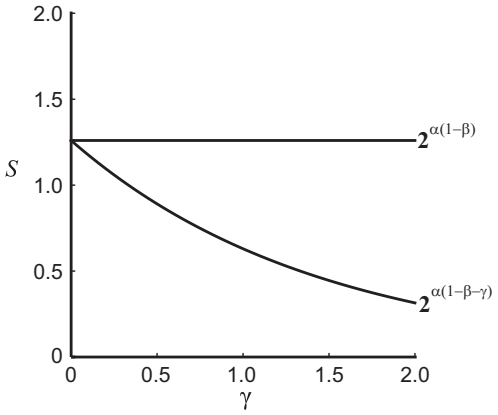

Fig. 1. The relative advantage of ploidy levels on the (γ, s) plane. Equations $s=2^{\alpha(1-\beta)}$ and $2^{\alpha(1-\beta-\gamma)}$ specify the boundaries between parameter regions separating areas in which haploidy and diploidy are advantageous. When $0<s<2^{\alpha(1-\beta-\gamma)}$, haploidy is always more advantageous than diploidy. When $2^{\alpha(1-\beta-\gamma)}<s<2^{\alpha(1-\beta)}$, diploidy is more advantageous than haploidy in nutrient-poor environments, but the opposite is true in nutrient-rich environments. When $2^{\alpha(1-\beta)}<s$, diploidy is always more advantageous than haploidy. Parameter values are $\alpha=1.0$, $\beta=2/3$.

is true in nutrient-rich environments. When $2^{\alpha(1-\beta)} < s$, diploidy is always more advantageous than haploidy.

3.2. Relative advantages of each ploidy when handling time is significant ($h_p > 0$)

We next consider the case in which the nutrient uptake rates are saturated because of a handling time. To simplify the model for analysis, we first consider the case when the density of nutrients N is very small and the case when it is very large. When $h_p > 0$, our results are affected by parameters in addition to s, α, β, γ; namely, the advantage of diploids in handling time efficiency over the haploids r, the handling time efficiency h_h, the mortality coefficient m_0, the initial cell size v_h, and the energy conversion efficiency e_h.

When N is very small, Eqs. (9a) and (9b) represents the boundary between the parameter regions where different ploidy levels are relatively advantageous:

$$s = 2^{\alpha(1-\beta-\gamma)} + \Delta_P, \tag{13}$$

where $\Delta_P := m_0 h_h \delta(\gamma)\left\{(2^{-\alpha\gamma}/r) - 2^{\alpha(1-\beta-\gamma)}\right\}/v_h^{\gamma} e_h$ and $\delta(\gamma) := (1-2^{-\gamma})/\gamma(\ln 2)$. When. $s > 2^{\alpha(1-\beta-\gamma)} + \Delta_P$ holds, diploidy is more advantageous than haploidy, but when the opposite inequality holds, $s < 2^{\alpha(1-\beta-\gamma)} + \Delta_P$, haploidy is more advantageous than diploidy (Appendix C).

When nutrient availability is very high, the boundary separating the regions of the different outcomes is given by the following equation:

$$s = (1/r) + \Delta_R, \tag{14}$$

where $\Delta_R := -m_0 h_h \delta(\gamma)(1-2^{-\alpha\gamma})/r v_h^{\gamma} e_h$. When $s > (1/r) + \Delta_R$, diploidy is more advantageous than haploidy, and when $s < (1/r) + \Delta_R$, haploidy is more advantageous than diploidy (Appendix C).

Intuitively, these results can be explained as follows: Under nutrient-poor condition, there is little effect of efficiency of handling time r because nutrient uptake rate linearly increase with nutrient level and generation time is almost independent of handling time. If $\alpha = 0$, diploids must be more efficient at using resources ($s > 1$) for advantage of diploids over the haploids because generation time and survivorship of both ploidy level should be identical without advantage for s. In the case where $\alpha > 0$, haploids tend to be advantageous over diploids because of a higher surface area to volume ratio when $0 < \beta < 1$. Especially diploid must have advantage of resource use ($s > 2^{\alpha(1-\beta)} > 1$) when $\gamma = 0$, but this boundary decrease with increasing of effect of cell size on mortality $\gamma > 0$ because the larger diploids have an advantage in survivorship over the smaller haploids. When nutrients are abundant (nutrient-rich condition), the phase with highest e_p/h_p ratio wins, because of assumption that a diploid cell is equivalent to two haploid cells when nutrients are abundant when $s = r = 1$.

Eqs. (13) and (14) suggest that the boundaries between parameter regions favoring different ploidy levels are determined by directions of the inequality describing the energy conversion efficiency level of diploids relative to that of haploids s, and the right-hand side terms of Eqs. (13) and (14) that consists of two terms: the first term is the power-of-two function for the exponents α, β, and γ, or the reciprocal of the handling time efficiency of

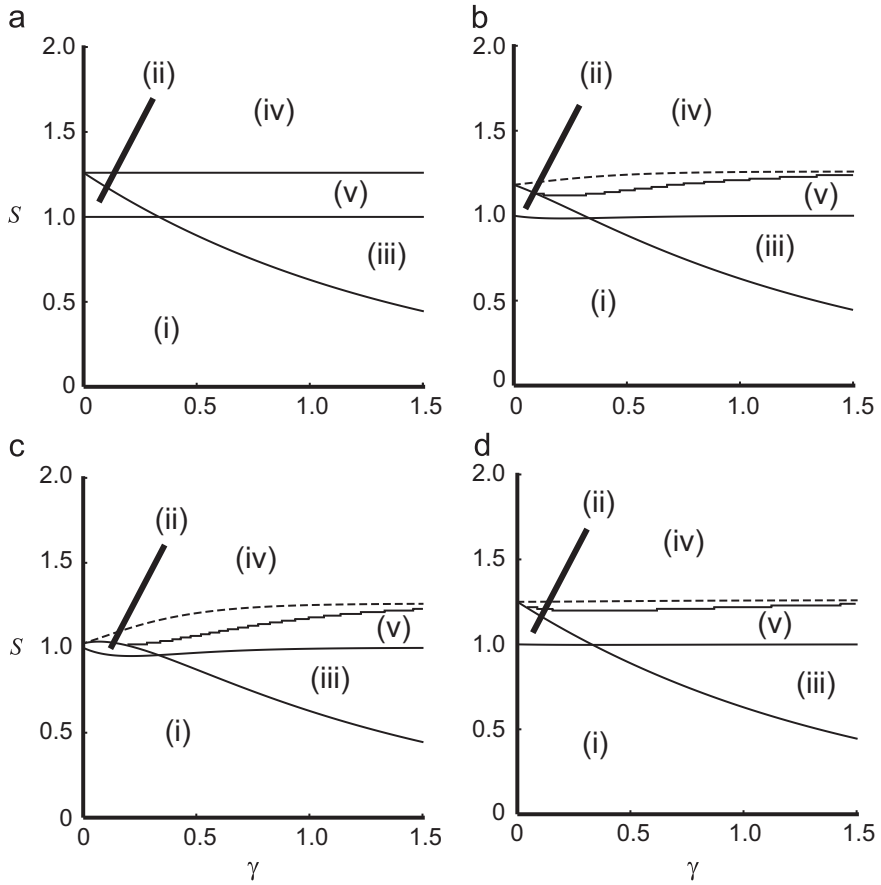

Fig. 2. The relative advantage of ploidy levels in the (γ, s) plane for different values of the life history parameters m_0, h_h, v_h, and e_h. The fitness advantage is judged from the relative values of the intrinsic population growth rates. Five patterns are observed. Here, conditions (i), (ii), and (iii) are defined by analytical results (solid lines), but the boundary between (iv) and (v) was only calculated numerically. Where the approximated boundaries do not coincide with the numerically calculated boundaries, dashed lines denote the approximated boundaries. (a) $m_0 h_h/e_h \approx 0$; (b) $m_0 h_h/e_h = 0.3$; (c) $m_0 h_h/e_h = 0.9$; (d) $v_h = 10$. Other parameters are $\alpha = 1.0$, $\beta = 2/3$, $r = 1.0$, $m_0 h_h/e_h \approx 0.036$, $\sigma = 0.73$, $v_h = 56$.

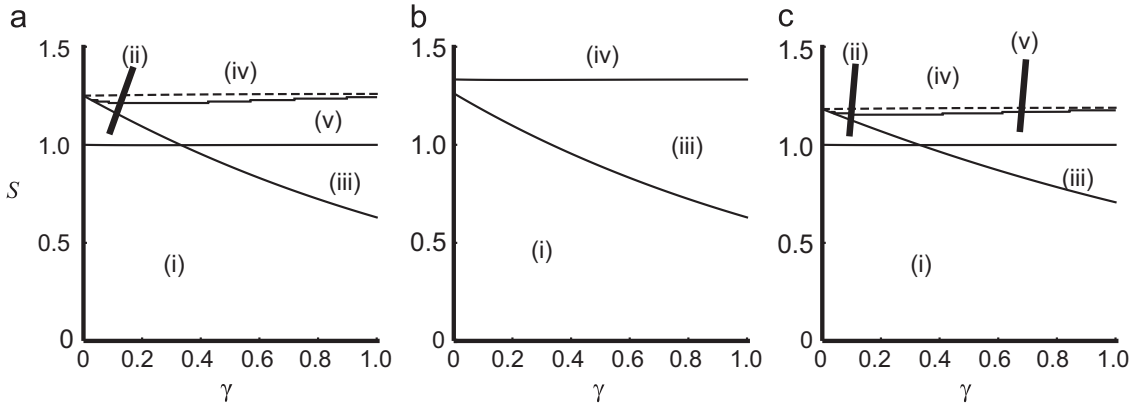

Fig. 3. The relative advantage of ploidy levels on the (γ, s) plane, calculated using different values of parameters α and r. The fitness criterion is the relative value of the intrinsic population growth rate. (a) $\alpha=1$ and $r=1$; (b) $\alpha=1$ and $r=0.75$; (c) $\alpha=0.75$ and $r=1$. Other parameters are: $\beta=2/3$, $m_0h_h/e_h\approx 0.036$, $\sigma=0.73$, $v_h=56$.

diploids relative to that of haploids, $1/r$, and the second term, which is due to the effect of the nonlinearity of the nutrient uptake rate, is proportional to $m_0h_h\delta(\gamma)/v_h^{\gamma}e_h$. Because the first term is larger than the second term in the plausible parameter space, and because $\phi_h>0$ is a necessary condition, $m_0h_h\delta(\gamma)/v_h^{\gamma}e_h<1$ (see Appendix C), the trade-off between s and the power-of-two function is more important than that between s and the second nonlinear term for determining the relative advantage of each ploidy level.

Fig. 2 illustrates parameter regions differing in the relative advantage of ploidy levels on the (γ, s) plane, calculated numerically using different values (estimated from the literature) for the life history parameters m_0, h_h, v_h, and e_h. Because the effect of cell size could be affected by γ on the plane, we checked the effect of cell size v_h separately from the effect of m_0h_h/e_h. The numerical results suggest there is no dominant difference between the effects of m_0h_h/e_h and v_h (Fig. 2(b) and (d)). As shown by the analytical results, in the case where the effect of the non-linear term is very weak (smaller m_0, smaller h_h, larger v_h, and larger e_h), we have the following regions (Fig. 2(a)): (i) haploidy is always advantageous over diploidy ($s<1/r$ when $1/r<2^{\alpha(1-\beta-\gamma)}$, or $s<2^{\alpha(1-\beta-\gamma)}$ when $1/r>2^{\alpha(1-\beta-\gamma)}$); (ii) haploidy is advantageous over diploidy under nutrient-poor conditions, and vice versa ($1/r<s<2^{\alpha(1-\beta-\gamma)}$ when $1/r<2^{\alpha(1-\beta-\gamma)}$); (iii) diploidy is advantageous over haploidy under nutrient-poor conditions, and vice versa ($2^{\alpha(1-\beta-\gamma)}<s<1/r$ when $2^{\alpha(1-\beta-\gamma)}<1/r$); and either (iv), diploidy is always advantageous over haploidy, or (v), diploidy is advantageous in both nutrient-poor and nutrient-rich conditions and haploidy is advantageous over diploidy when nutrient availability has an intermediate value ($s>2^{\alpha(1-\beta-\gamma)}$ when $1/r<2^{\alpha(1-\beta-\gamma)}$, or $s>1/r$ when $1/r>2^{\alpha(1-\beta-\gamma)}$). When either (iv) or (v) is realized, the boundary is close to $s\approx 2^{\alpha(1-\beta)}$, although we cannot derive it analytically (Appendix C). As the effect of the nonlinear term increases (i.e., larger m_0, larger h_h, smaller v_h, and smaller e_h), the boundaries between regions of relative advantage of the ploidy levels change from the above simple functions (Fig. 2(b)–(d)), especially for smaller γ. When the nonlinear term is very large, the area of region (ii) becomes very small (Fig. 2(c)), because both boundaries $2^{\alpha(1-\beta-\gamma)}+\Delta_P$ and $(1/r)+\Delta_R$ approach $1/r$ when $m_0h_h\delta(\gamma)/v_h^{\gamma}e_h=1$ and $\gamma=0$.

Figs. 3 and 4 illustrates the parameter regions showing regions of different relative advantages of ploidy levels on the (γ, s) plane numerically calculated with different values for exponent α in the power-of-two function or for the relative handling time efficiency of diploids to haploids r. Here, the existence of region (ii), in which haploidy is advantageous over diploidy under nutrient-poor conditions and vice versa, strongly depends on the efficiency of the handling time r. When the handling time efficiency of diploids is equivalent to haploids ($r=1$), region (ii) always exists on the plain (Fig. 3(a) and (c), because $2^{\alpha(1-\beta)}>1$ for any $\alpha>0$. But the area of region (ii) decreases with decreasing r and the region disappears when $2^{\alpha(1-\beta)}<1/r$ (Fig. 3(b)). When neither the handling time efficiency ($r=1$) nor the mortality ($\gamma=0$) differs between different cell sizes, region (ii) always exists, because $2^{\alpha(1-\beta)}>1$ for any $\alpha>0$. Here, we can calculate the necessary condition for r as $r>1/2^{\alpha(1-\beta)}$. When region (ii) exists, the intersection on the plain is given by $\gamma^*=1-\beta+(\ln r/\alpha\ln 2)$ and the range of s in the region (ii) $\{1-(m_0h_h\delta(\gamma)/v_h^{\gamma}e_h)\}\left\{2^{\alpha(1-\beta-\gamma)}-(1/r)\right\}$ becomes greater when $\gamma<1-\beta$, but shorter when $\gamma>1-\beta$, as exponent α increases. Especially when $r=1$ and nonlinear term is very small, the area of region (ii) is always greater with increasing of α when $\gamma<\gamma^*=1-\beta$ (Fig. 4).

3.3. Relative advantage of different ploidy under density dependence

In this section, we consider the relative advantage of different ploidys in a density-dependent population. Here, the relative advantage of the different ploidy levels is judged by which one outcompetes the other when the population is at equilibrium. With the population dynamics given by Eqs. (10a) and (10b) and the nutrient levels given by Eq. (11), the model leads to three clear conclusions (Appendix D): First, haploid and diploid types never coexist. Second, the boundary separating the parameter regions determining the winning type is described by the equation $s=2^{\alpha(1-\beta-\gamma)}+\Delta_P$ (see Eq. (13)). When $s>2^{\alpha(1-\beta-\gamma)}+\Delta_P$, the diploid abundance D reaches the carrying capacity and the haploid abundance H goes to zero. In contrast, when $s<2^{\alpha(1-\beta-\gamma)}+\Delta_P$, the haploid abundance H reaches the carrying capacity and the diploid abundance D goes to zero. Third, the position of the boundary depends on the energy conversion and handling time efficiency levels of the diploids compared to those of the haploids (s and r), the scaling of cell size with nuclear content and of mortality with cell size α and γ, energy conversion efficiency e_h, mortality coefficient m_0, initial cell volume v_h, and handling time efficiency h_h. Note that the position of the boundary is independent of the nutrient capture rate σ, the nutrient concentration in the inflowing medium N_0, and the decay rate f_{decay}.

In a density-dependent population, the boundary between the two regions of different relative advantage is the same as the boundary under density independence with nutrient-poor conditions. This means that the ploidy level with the higher nutrient usage efficiency N_p^* is advantageous and its competitor is excluded (See Appendix C). At nutrient equilibrium, the disadvantageous ploidy level never invades the population because at the

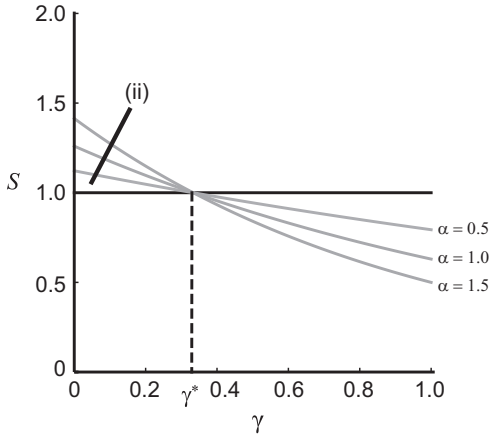

Fig. 4. Change in region (ii) with different values of exponent α when $=1$. Black line indicates boundary for nutrient-rich condition $1/r$ and gray lines indicate boundary for nutrient-poor condition $2^{\alpha(1-\beta-\gamma)}$ for different α. The intersection is $\gamma^*=1-\beta$ and the area of region (ii) always greater with larger value of α when $\gamma<\gamma^*$. Other parameters are: $\beta=2/3$ and $m_0h_h/e_h=0$.

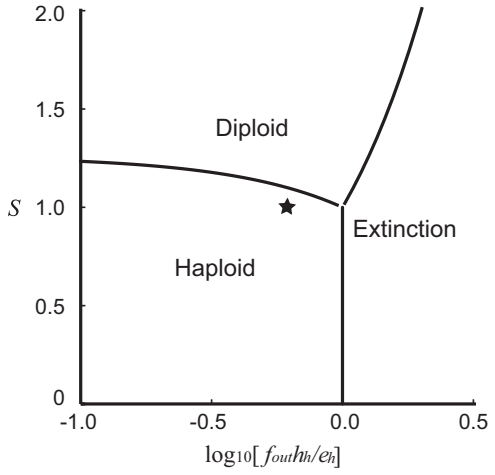

Fig. 5. The relative advantage of ploidy levels in a chemostat at equilibrium. The $(\log_{10}[f_{out}h_h/e_h], s)$ plane is divided into three regions: in the haploid region, haploids reach their carrying capacity and diploids become extinct ($\overline{H}>0$ and $\overline{D}=0$); in the diploid region, diploids reach their carrying capacity and haploids become extinct ($\overline{H}=0$and $\overline{D}>0$); and in the extinction region, both haploids and diploids become extinct ($\overline{H}=0$ and $\overline{D}=0$). The star indicates the parameter set used in the competition experiment of Adams and Hansche (1974). We used the following parameter values: $\alpha=1.0$, $\beta=2/3$, $s=1.0$, $r=1.0$, $v_h=56$, $h_h=22.09$, $e_h=6.13$, and $f_{out}=0.17$.

equilibrium nutrient level, the invader's population growth rate is negative. Further, this relative advantage is independent of the nutrient inflow N_0 and decay f_{decay} rates, because the efficiency of nutrient usage is decided by microbial characteristics, independently of environmental factors.

3.4. Chemostat model

When both haploid and diploid cells are cultured in a chemostat, the population dynamics corresponds to the model described in Section 2.3 (Appendix E) with $\gamma=0$ and $m_0=f_{out}$. The model predicts that the relative advantage of a given ploidy level depends on the outflow rate f_{out}. Fig. 5 illustrates the relative advantage of each ploidy level in the $(\log_{10}[f_{out}h_h/e_h], s)$ plane using different parameter values estimated from the literature (Appendix F). In the figure, boundaries are given by putting $m_0=f_{out}$ and $\gamma=0$ into Eq. (13), (C.5a), and (C.5b). The figure shows that the relative advantage the ploidy levels in a nutrient-poor environment can be reversed by increasing the outflow rate f_{out}. When $1/r<2^{\alpha(1-\beta)}$, haploid cells are dominant over diploid cells with weak outflow whereas diploids are dominant over haploids with strong outflow. This result suggests that the predictions of the nutrient-limitation hypothesis can be detected when nutrient conditions and population sizes are both strongly controlled by the outflow rate in the chemostat.

4. Discussion

We studied the relative advantage of haploid versus diploid microbes as predicted by ecophysiological hypotheses. To measure the relative advantage of the ploidy levels, we adopted two different fitness metrics: one based on the intrinsic population growth rate and the other based on the equilibrium state of density-dependent population dynamics.

The results of both analyses suggested that the boundary determining which ploidy level has the relative advantage can be understood in terms of a trade-off between the energy conversion efficiency level of diploids relative to that haploids (s) and an expression consisting of two terms. The first term depends on the exponents for cell size (α) and the scaling of mortality with cell size (γ), or the handling time efficiency of diploids relative to that of haploids (r). The second term is proportional to handling time efficiency (h_h) and mortality coefficient (m_0), and inversely proportional to a power function of cell size (v_h) and the energy conversion efficiency (e_h). However, because the value of the first term is larger than the absolute value of the second term in the plausible parameter space, the trade-off between s and the power-of-two function (the first term) essentially determines the relative advantage of the ploidy levels. Hence, we here discuss the relative advantage of the ploidy levels in relation to the first term.

4.1. Relative advantage of ploidy level

In density-independent models, the intrinsic population growth rate is the fitness metric. We thus searched for the necessary conditions for a parameter region to exist consistent with the nutrient-limitation hypothesis. First, if the nutrient uptake rate is linear ($h_p=0$), there is no region in which haploidy is only advantageous over diploidy under nutrient-poor conditions (Fig. 1). Second, if the microbial nutrient uptake rate is nonlinear ($h_p>0$), five different patterns are possible. In particular, haploidy is advantageous over diploidy under nutrient-poor conditions, and vice versa, when the conditions $1/r<s<2^{\alpha(1-\beta-\gamma)}$ and $1/r<2^{\alpha(1-\beta-\gamma)}$ are satisfied (region (ii) in Fig. 2(a)).

In density-dependent populations, the fitness advantage is decided by the equilibrium population dynamics. Haploid and diploid microbes never coexist; rather, there is a boundary $s=2^{\alpha(1-\beta-\gamma)}$ separating the parameter regions in which the different ploidy levels are advantageous. This boundary is the same as the boundary in the density-independent models under nutrient-poor conditions, and it is independent of the amount of nutrient inflow N_0. Because in the population dynamics, exploitative competition for a single nutrient tends to select for the species that has the highest nutrient usage efficiency, the advantageous ploidy level is the one that is advantageous in nutrient-poor environments when the nutrient level is fixed.

Our results suggest that the energy conversion efficiency and the handling time efficiency of diploids relative to haploids s and r, and the exponents of the power-of-two function α and γ, are critical. These parameters reflect the trade-off between the effects of increasing (to diploid) or decreasing (to haploid) the genome size: Haploids have a higher nutrient uptake efficiency and a rapid doubling rate because of their higher surface area to volume ratio,

whereas diploids benefit from the higher gene dosage and smaller size-dependent mortality conferred on them by their larger cell size.

4.2. Nutrient limitation hypothesis

The parameters s and r are a measure of ploidy-dependent gene regulation, or the activities of particular enzymes (gene dosage effect), and also of the cost of DNA production from phosphorus in the cell. In higher eukaryotic species, the level of expression or repression of an autosomal gene and the activities of enzymes are often proportional to the ploidy level (DeMaggio and Lambrukos, 1974; Guo et al., 1996; Suzuki et al., 1999; Timko et al., 1980).

The nutrient-limitation hypothesis assumes $s \approx 1$ and $r \approx 1$, because although twice as much DNA in the diploid cell means twice the transcription of mRNA, this advantage is canceled out by its doubled volume (Perrot, 1994). In fact, Adams and Hansche (1974) reported no significant difference in doubling time between haploid and diploid cells under nutrient-rich conditions, a result consistent with the assumptions of the nutrient-limitation hypothesis (See Appendix F). In addition, the exponent of cell size α is often estimated to be approximately one (Gregory, 2001). From these values, we can calculate the necessary conditions for the evolutionary stability of unicellular diploidy.

Because the ploidy level with the higher usage efficiency is advantageous and its competitor is excluded (Appendix C), the boundary for relative advantage of ploidy level with nutrient dynamics is determined by Eq. (13). Considering dominant term $2^{\alpha(1-\beta-\gamma)}$, our model implies that the relative advantage of ploidy levels is strongly determined by whether or not the efficiency s is larger than $2^{\alpha(1-\beta-\gamma)}$. When the mortality is independent of size ($\gamma = 0$), the efficiency of diploids must be greater than that of haploids in order to maintain diploidy, because $2^{\alpha(1-\beta)} > 1$. For example, diploids must have about a 1.26 fold advantage over haploids for s for typical parameter sets, $\alpha = 1$ and $\beta = 2/3$. However if there is strong size-dependent mortality ($\gamma > 0$), diploidy is also more likely to be advantageous over haploidy without an advantage for s (e.g., diploids are advantageous over the haploids when $s = 1$ and $\gamma > 1/3$).

In contrast, smaller haploids tend to have an advantage over diploids when $\gamma < 0$, because $2^{\alpha(1-\beta-\gamma)}$ increases exponentially with decreasing γ. In this paper, we assumed that the unknown exponent for the scaling of mortality with cell size γ satisfied $0 < \gamma \leq 1$, because mortality decreases as cell size, or the investment in defensive substances, increases. However, if some factor exists that causes large individuals to suffer from higher mortality (e.g., a size-dependent discovery rate by predators or size-dependent damage by UV light), the relative advantage of haploidy over diploidy would be increased.

Therefore, from our analysis, we conclude that either size-dependent mortality or an advantage of diploidy with regard to energy conversion efficiency into cell structure, or both, are necessary for diploid microbes to succeed. The nutrient-limitation hypothesis assumes that the ability of diploids to produce twice as many gene products is canceled out by their doubled volume. When cell size linearly increases with ploidy level ($\alpha = 1$) as nutrient-limitation hypothesis assumes, the relative amount of gene product for cell size of diploids could be calculated as $2/2^{\alpha} = 1$. This is the mathematical description that the relative ability of diploids is equivalent for haploids. However relative ability of diploids can be greater than haploids ($2/2^{\alpha} > 1$) if the size of a diploid cell is smaller than twice size of haploid cell ($0 < \alpha < 1$). For example, Weiss et al. (1975) reported that the volume of diploid yeast cells is 1.57 times the volume of haploid cells ($\alpha \approx 0.66$). If the volume of the diploid cell can be smaller than the volume of two haploid cells and the relative ability of diploids s is consistent with relative amount of gene product for cell size $2/2^{\alpha}$ for haploids ($\alpha < 1$ and $s = 2/2^{\alpha}$), then the relative advantage of the energy conversion efficiency s can be greater than one. As a result, the exception of allometric relationship between ploidy level and cell size can accelerate the advantage of diploidy over haploidy in spite of the smaller surface to volume ratio of the latter and the increased cost of DNA to the former (e.g., $2/2^{\alpha} \approx 1.27$ is larger than $2^{\alpha(1-\beta-\gamma)} \approx 1.16$ for $\alpha = 0.66$, $\beta = 2/3$ and $\gamma = 0$).

4.3. Comparison with empirical observations

Lewis (1985) hypothesis, that haploids enjoy an advantage in nutrient-poor environments, whereas in nutrient-rich environments diploids can hold their own or may have an advantage over haploids (Perrot, 1994), is often favored by researchers studying the evolution of ploidy (Coelho et al., 2007; Mable and Otto, 1998; Otto and Gerstein, 2008; Perrot, 1994). The results of our research support this hypothesis in part.

We found that when nutrient availability is fixed and populations grow exponentially, the intrinsic rate of population growth of the two ploidy levels can be reversed by a change in nutrient availability (region (ii) in Fig. 2). However, when population size is regulated by mortality and explicit nutrient dynamics is considered in wild environment, the relative advantage of the two ploidy levels is independent of the amount of nutrient inflow into a mixed medium, even though the smaller haploid is assumed to have a higher nutrient uptake efficiency. The difference between our results and those predicted by the nutrient-limitation hypothesis is due to the life history processes and population dynamics of the microbes.

The nutrient-limitation hypothesis is supported by the results of culturing experiments with the budding yeast *S. cerevisiae* carried out in chemostats (Adams and Hansche, 1974). They found that the maximum reproductive rates of haploid and diploid cells assayed in two completely different sets of environmental conditions were not significantly different when all nutrients were present in excess. They also measured the ability of haploids to increase their frequency in a culture, after being introduced at a frequency of 10% of the resident strain, when their growth was limited by nutrient scarcity. They found that the frequency of the haploids significantly increased in organic phosphate-limited chemostats. However, they could not detect any significant increase in the haploid frequency in chemostats with other nutrient limitations (dextrose or inorganic phosphate).

These observations are partially consistent with our model's predictions. When the maximum reproductive rates of the two ploidy levels are almost the same, we expect the enegy conversion efficiency s to be $s \approx 1$ when $\alpha \approx 1$ and $r \approx 1$. Our model predicts that haploidy is always advantageous over diploidy at population equilibrium in a chemostat (star in Fig. 5). Thus, our model explains why the frequency of haploids increases in nutrient-limited chemostats, but it cannot explain why the frequency does not always increase.

This discrepancy between the model prediction and the experimental results can be explained in three ways. First, in these experiments, the relative advantage of a given ploidy level was not measured at equilibrium but by a change in its frequency, and the increase in frequency of the haploid strain was very small (the average difference in the reproductive rate was estimated to be 0.006). Thus, the difference in the population growth rate between haploids and diploids caused by this ecophysiological factor might be too small to detect on the time scale of the experiments. Second, our model assumes that the nutrient uptake rate is regulated by surface area under nutrient-poor conditions. However, if the nutrient uptake rate is always regulated by cell volume, the same fitess would be observed in diploid and haploid populations under all nutrient densities (Appendix A). Weiss et al. (1975)

reported that in budding yeast the relative activities of internal cellular enzymes are regulated by cell volume but that cell surface enzymes are often regulated by cell surface area. They concluded that haploidy is advantageous over diploidy when fitness is determined by the activities of cell surface enzymes, but that diploids should have the same fitness as haploids when fitness is determined by the activities of internal enzymes. The experimental results can be explained if the nutrient uptake activity is regulated by a cell surface enzyme in an organic phosphate-limited medium but by an internal enzyme in other media.

Third, it is possible that other factors differ between ploidy levels. For example, it is known that *S. cerevisiae* is normally diploid. The genomic convergence toward diploidy shown experimentally in *S. cerevisiae* (Gerstein et al., 2008, 2006) might be an effect of its speed of adaptation to new environments (Paquin and Adams, 1983). Also, the results of experiments testing the nutrient-limitation hypothesis in unicellular yeasts are mixed (Glazunov et al., 1989; Mable and Otto, 1998; Naĭdhardt and Glazunov, 1991). This mixed outcome might be explained by our model. Our research illustrates the importance of explicitly modeling experimental systems to improve out understanding of the evolution of life cycles.

Acknowledgments

We thank H. Hakoyama, M. Hori, S. Kawaguchi, S. Shimada, and J. Urabe for valuable information and very helpful comments. We are very grateful to Sarah P. Otto for helpful comments and critical readings of the manuscript. This work was supported by a Grant-in-Aid for Japan Society for the Promotion of Science (JSPS) fellows to KB (no. 10J00368), a Grant-in-Aid for a JSPS postdoctoral fellow for research abroad to KB, and a Grant-in-Aid for Scientific Research (B) to YI (nos. 24370011 and no. 15H04423). We gratefully acknowledge the critical reviews by three anonymous reviewers.

Appendix A. Intrinsic rate of population growth rate in microbial life cycle

A.1. Generation time T_p

Substituting Eq. (3) into Eq. (1a), we get a differential equation describing cellular volume:

$$\frac{dV_p}{d\tau}=\frac{e_p\sigma {V_p}^{\beta}N}{1+h_p\sigma {V_p}^{\beta-1}N} \text{ for } 0\le\tau\le T_p \tag{A.1}$$

with boundary conditions $V_p(0)=v_p$ and $V_p(T_p)=2V_p(0)$, where T_p is generation time. By integrating Eq. (A.1) with separation of variables, we can derive the generation time:

$$T_p=\frac{\left(2^{1-\beta}-1\right){v_p}^{1-\beta}}{(1-\beta)e_p\sigma N}+\frac{h_p(\ln 2)}{e_p}. \tag{A.2}$$

Note that from Eq. (A.2), we can predict that the generation time is proportional to $G_p^{\alpha(1-\beta)}$ when $h_p=0$. Previously, Cavalier-Smith (1978) predicted that cell cycle length is proportional to the 1/3 power of genome size, because the length should be proportional to cell volume and inversely proportional to nuclear surface area and both geometries are related to genome size. In the above formalism, this relationship holds when $\alpha=1$ and $\beta=2/3$.

A.2. Survivorship $L_p(T_p)$

Substituting Eq. (5) into Eq. (4a), we get a differential equation describing survival to age τ:

$$\frac{dL_p}{d\tau}=-\frac{m_0}{V_p^{\gamma}}L_p, \tag{A.3}$$

for the initial condition $L_p(0)=1$. By integrating Eq. (A.3), we can derive the survivorship of one generation

$$L_p(T_p)=\begin{cases}\exp\left[-\frac{m_0{v_p}^{1-\beta-\gamma}\left(2^{1-\beta-\gamma}-1\right)}{e_p\sigma(1-\beta-\gamma)N}-\frac{m_0h_p{v_p}^{-\gamma}(1-2^{-\gamma})}{e_p\gamma}\right] & (1-\beta-\gamma\neq 0,\ \gamma\neq 1)\\ \exp\left[-\frac{m_0\left(2^{1-\beta-\gamma}-1\right){v_p}^{1-\beta-\gamma}}{e_p\sigma N(1-\beta-\gamma)}-\frac{m_0h_p(\ln 2)}{e_p}\right] & (1-\beta-\gamma\neq 0,\ \gamma=1)\\ \exp\left[-\frac{m_0(\ln 2)}{e_p\sigma N}-\frac{m_0h_p{v_p}^{-\gamma}(1-2^{-\gamma})}{e_p\gamma}\right] & (1-\beta-\gamma=0,\ \gamma\neq 1)\end{cases}. \tag{A.4}$$

The limiting cases ($\gamma=1$ and $1-\beta-\gamma=0$) in Eq. (A.4) can be determined by taking the limit of the first equation. Thus, these limiting cases are subsumed into the first case and we do not have to calculate them separately.

A.3. Intrinsic population growth rate ϕ_p

The intrinsic rate of population increase for a unicellular organism with binary fission is given as follows (e.g.Irie et al., 2010):

$$\phi_p=\frac{\ln[2\times L(T_p)]}{T_p}. \tag{A.5}$$

By substituting Eq. (A.2) into Eq. (A.5), we can derive the intrinsic population growth rate ϕ_p as Eq. (6) in the text. Then, by substituting Eq. (7) and Eqs. (8a) and (8b) into Eq. (6), we can derive Eqs. (9a) and (9b), where the constants are $C_1:=(1-\beta)e_h\sigma(\ln 2)>0$, $C_2:=\left(2^{1-\beta}-1\right)v_h^{1-\beta}>0$, $C_3:=(1-\beta)\sigma(\ln 2)>0$, $C_4:=\frac{\left(2^{1-\beta-\gamma}-1\right)v_h^{1-\beta-\gamma}}{(1-\beta-\gamma)e_h\sigma(\ln 2)}$, and $C_5:=\frac{(1-2^{-\gamma})}{\gamma v_h^{\gamma}e_h(\ln 2)}$ (C_4 and C_5 are positive when $\gamma>0$).

A.4. Average nutrient uptake rate $\tilde{U}_p$

By performing a transformation of the independent variable from τ to V based on Eqs. (1a) and (1b), we obtain the average nutrient uptake as

$$\tilde{U}_p=\frac{1}{e_pT_p}\int_{v_p}^{2v_p}L(V_p)dV_p. \tag{A.6}$$

When the effect of mortality is very weak ($m_0\approx 0$), we have the analytical result

$$\tilde{U}_p=\frac{1}{T_p}\int_{v_p}^{2v_p}\frac{1}{e_p}dV_p=\frac{v_p}{e_pT_p}=\frac{(1-\beta)v_p\sigma N}{\left(2^{1-\beta}-1\right){v_p}^{1-\beta}+h_p(\ln 2)(1-\beta)\sigma N}, \tag{A.7}$$

and substituting Eq. (A.6) into Eq. (11), we obtain

$$N_0 f_{in} - \tilde{N} f_{decay} - \frac{C_6 \tilde{N}}{C_2 + h_h C_3 \tilde{N}} H - \frac{2^{\alpha} C_6 \tilde{N}}{2^{\alpha(1-\beta)} C_2 + h_d C_3 \tilde{N}} D = 0 \tag{A.8}$$

with the positive constant $C_6 := (1-\beta) v_h \sigma$.

We next show that Eq. (11) has only one stable solution $\tilde{N}$ when $N > 0$. When the nutrient level is very low ($N \approx 0$), the nutrient uptake rate should be zero ($\tilde{U}_p = 0$) and the sign of dN/dt will be positive because of very low nutrient uptake and survivorship with small cell size and very large generation time ($dN/dt = N_0 f_{in} > 0$). And because we can treat $\tilde{U}_p$ as the function of nutrient density N, we have

$$\begin{aligned} \frac{d\tilde{U}_p}{dN} &= \frac{1}{e_p}\left\{ \left(\frac{d}{dN}\frac{1}{T_p}\right) \int_{v_p}^{2v_p} L_p(V_p) dV_p + \frac{1}{T_p}\left(\frac{d}{dN}\int_{v_p}^{2v_p} L_p(V_p) dV_p\right) \right\} \\ &= \frac{1}{e_p}\left\{ -\frac{1}{T_p^2}\frac{dT_p}{dN} \int_{v_p}^{2v_p} L_p(V_p) dV_p + \frac{1}{T_p}\left(\frac{d}{dN}\int_{v_p}^{2v_p} L_p(V_p) dV_p\right) \right\}, \end{aligned} \tag{A.9}$$

and Eq. (A.9) is positive because of $dT_p/dN < 0$, $\int_{v_p}^{2v_p} L_p(V_p) dV_p > 0$ and $\frac{d}{dN}\int_{v_p}^{2v_p} L_p(V_p) dV_p > 0$. Hence we have

$$\frac{d}{dN}\left(\frac{dN}{dt}\right) = -f_{decay} - H\frac{d\tilde{U}_h}{dN} - D\frac{d\tilde{U}_d}{dN} < 0, \tag{A.10}$$

and conclude that Eq. (11) has only one stable solution $\tilde{N}$ for $N > 0$.

2.5. Alternative mode of the nutrient uptake function U_p

In this article, we assumed that the nutrient uptake rate could be denoted as Eq. (3), that is, as proportional to the surface area under nutrient-poor conditions, but proportional to volume under nutrient-rich conditions. To check how the mode of the nutrient uptake function U_p affects our results, we show similar results with other functions of nutrient uptake. Here we show three types of function.

First, if handling time is independent of cell volume $\hat{h}_p := h_p$, then generation time and survivorship are given as

$$T_p = \frac{\left(2^{1-\beta}-1\right) {v_p}^{1-\beta}}{(1-\beta) e_p \sigma N} + \frac{h_p v_p}{e_p}, \tag{A.11a}$$

$$L_p(T_p) = \exp\left[-\frac{m_0\left(2^{1-\beta-\gamma}-1\right) v_p^{1-\beta-\gamma}}{e_p \sigma N (1-\beta-\gamma)} - \frac{m_0 h_p \left(2^{1-\gamma}-1\right) v_p^{1-\gamma}}{e_p (1-\gamma)} \right]. \tag{A.11b}$$

From Eqs. (A.11a) and (A.11b), we can derive the boundary for the relative advantage of haploids and diploids. When the effect of the non-linear term is very weak (smaller m_0, smaller h_h, larger v_h and larger e_h), the boundary is $s \approx 2^{\alpha(1-\beta-\gamma)}$ under nutrient-poor conditions and $s \approx 2^{\alpha}/r$ under nutrient-rich conditions.

Second, if we assume that the handling time is inversely proportional to the cell surface, that is, $\hat{h}_p := h_p / V_p^{\beta}$, where the nutrient uptake rate is always proportional to surface area, then the generation time and survivorship are

$$T_p = \frac{(1+h_p\sigma N)\left(2^{1-\beta}-1\right) {v_p}^{1-\beta}}{(1-\beta) e_p \sigma N}, \tag{A.12a}$$

$$L_p(T_p) = \exp\left[-\frac{m_0 (1+h_p\sigma N)\left(2^{1-\beta-\gamma}-1\right) v_p^{1-\beta-\gamma}}{(1-\beta-\gamma) e_p \sigma N} \right]. \tag{A.12b}$$

From Eqs. (A.12a) and (A.12b), we can derive an approximate boundary for the relative advantage of haploids and diploids of $s \approx 2^{\alpha(1-\beta-\gamma)}$ under nutrient-poor conditions and of $s \approx 2^{\alpha(1-\beta)}/r$ under nutrient-rich conditions.

Third, if we assume $U_p := \sigma V_p N / 1 + \hat{h}_p \sigma V_p N$ and $\hat{h}_p := h_p / V_p$, where the nutrient uptake rate is always proportional to volume, then the generation time and survivorship are

$$T_p = \frac{(1+h_p\sigma N)(\ln 2)}{e_p \sigma N}, \tag{A.13a}$$

$$L_p(T_p) = \exp\left[-\frac{m_0 (1+h_p\sigma N)\left(1-2^{-\gamma}\right) v_p^{-\gamma}}{\gamma e_p \sigma N} \right]. \tag{A.13b}$$

From Eqs. (A.13a) and (A.13b), we can derive the approximate boundary for the relative advantage of haploids and diploids as $s \approx 2^{-\alpha\gamma}$ under nutrient-poor conditions and as $s \approx 1/r$ under nutrient-rich conditions.

As shown by our analytical results (Appendix C), when the effect of the non-linear term is very weak, five patterns of results similar to the results obtained by assuming Eq. (3) are observed with convenient parameters. However, when $s=1$ and $r=1$, no region exists in which haploidy is advantageous over diploidy under nutrient-poor conditions, and vice versa. Hence, we assume Eq. (3) with $\hat{h}_p := h_p / V_p$ for our model to explain the logic of the nutrient-limitation hypothesis.

Appendix B. Relative advantage of haploids and diploids when $h_p = 0$

When $h_p = 0$, the growth rates of haploids and diploids, given by Eq. (6), become

$$\phi_h = \frac{C_1 N}{C_2} - \frac{m_0 C_1 C_4}{C_2}, \tag{B.1a}$$

$$\phi_d = \frac{s C_1 N}{2^{\alpha(1-\beta)} C_2} - \frac{m_0 2^{\alpha(1-\beta-\gamma)} C_1 C_4}{2^{\alpha(1-\beta)} C_2}. \tag{B.1b}$$

We can determine the relative advantage of different ploidy levels by examining the relative values of the slopes and intercepts of Eqs. (B.1a) and (B.1b), because fitness is a linear function of nutrient availability N.

The intercept for diploids is larger than that for haploids across the entire γ–s parameter space, because $2^{\alpha(1-\beta-\gamma)}/2^{\alpha(1-\beta)}$ is smaller than 1 when $\gamma > 0$. The slope of the diploid curve is larger than that of the haploid curve when $s > 2^{\alpha(1-\beta)}$; in this case, diploids always grow faster than haploids.

When $s < 2^{\alpha(1-\beta)}$, the growth rate curves intersect at the nutrient level $N^* = m_0 C_4 \left(2^{\alpha(1-\beta)} - 2^{\alpha(1-\beta-\gamma)}\right) / \left(2^{\alpha(1-\beta)} - s\right) > 0$. The value of growth rate at the intersection of the population growth rate curves is calculated as $\{m_0 C_1 C_4 (s - 2^{\alpha(1-\beta-\gamma)})\} / \left\{C_2 \left(2^{\alpha(1-\beta)} - s\right)\right\}$, and its sign is decided by the position of the boundary $s = 2^{\alpha(1-\beta-\gamma)}$.

From these calculations, we can conclude that in our system there are only three patterns of the relative advantage of haploids and diploids: (i) haploidy is always advantageous over diploidy when $0 < s < 2^{\alpha(1-\beta-\gamma)}$; (ii) diploidy is advantageous over haploidy under nutrient-poor conditions, and vice versa, when $2^{\alpha(1-\beta-\gamma)} < s < 2^{\alpha(1-\beta)}$; and (iii) diploidy is always advantageous over haploidy when $2^{\alpha(1-\beta)} < s$ (Fig. 1).

Appendix C. Relative advantage of haploids and diploids when $h_p > 0$

C.1. Relative advantage of ploidy by relative fitness when $N << C_2/h_p C_3$

When the density of nutrients is sufficiently low, the growth rates of haploids and diploids given by Eqs. (9a) and (9b) become

$$\phi_h \approx \frac{C_1 N}{C_2} - \frac{m_0 h_h C_1 C_5 N}{C_2} - \frac{m_0 C_1 C_4}{C_2}, \tag{C.1a}$$

$$\phi_d \approx \frac{sC_1N}{2^{\alpha(1-\beta)}C_2} - \frac{2^{-\alpha\gamma}m_0h_hC_1C_5N}{r2^{\alpha(1-\beta)}C_2} - \frac{m_0 2^{\alpha(1-\beta-\gamma)}C_1C_4}{2^{\alpha(1-\beta)}C_2}. \quad \text{(C.1b)}$$

Again, we can assess the relative advantages of ploidy levels from the slopes and intercepts of Eqs. (C.1a) and (C1b), because fitness is a linear function of N.

The intercept for diploids is larger than that for haploids across the entire γ–s parameter space, because $2^{\alpha(1-\beta-\gamma)}/2^{\alpha(1-\beta)} < 1$ when $\gamma > 0$. The slope for diploids is larger than that for haploids when $s > 2^{\alpha(1-\beta)} + m_0h_hC_5\left\{(2^{-\alpha\gamma}/r) - 2^{\alpha(1-\beta)}\right\}$. The equation for the boundary can be rewritten as

$$s = 2^{\alpha(1-\beta)} + m_0h_h\delta(\gamma)\left\{(2^{-\alpha\gamma}/r) - 2^{\alpha(1-\beta)}\right\}/v_h^{\gamma}e_h. \quad \text{(C.2)}$$

However, this calculation of the relative advantage of ploidy levels is not appropriate for nutrient-poor conditions because this approximation includes the case with $\phi_p < 0$. Thus, we need to consider the case of $\phi_p > 0$.

C.2. Relative advantage of ploidy determined by relative fitness under nutrient-poor conditions

The nutrient usage efficiency N_p^* is that at which $\phi_p = 0$ and is

$$N_h^* = \frac{m_0C_4}{1 - m_0h_hC_5}, \quad \text{(C.3a)}$$

$$N_d^* = \frac{m_0 2^{\alpha(1-\beta-\gamma)}C_4}{s - m_0h_h(2^{-\alpha\gamma}/r)C_5}. \quad \text{(C.3b)}$$

When $N = N_p^* + \varepsilon$, where ε has a small positive value, the population growth rate of the diploids or haploids should be positive. Hence, the relative advantage of the ploidy levels is determined by the relative value of N_p^*. Setting $N_h^* = N_d^*$ yields the boundary condition Eq. (13). Because N_p^* depends strongly on the survivorship of the microbe, the dominant term in Eq. (13) can be derived as $\ln[L_d(T_d)]/\ln[L_h(T_h)] \approx 2^{\alpha(1-\beta-\gamma)}/s$.

C.3. Relative advantage of ploidy determined by relative fitness under nutrient-rich conditions

When the density of nutrients is very large, Eqs. (9a) and (9b) converge to maximum population growth rates

$$\phi_h^{max} := \frac{C_1}{h_hC_3}(1 - m_0h_hC_5), \quad \text{(C.4a)}$$

$$\phi_d^{max} := \frac{C_1}{h_hC_3(1/r)}\{s - m_0h_hC_5(2^{-\alpha\gamma}/r)\}. \quad \text{(C.4b)}$$

Setting $\phi_h^{max} = \phi_d^{max}$, we can derive boundary condition given by Eq. (14). The dominant term in Eq. (14) can be derived as $T_d/T_h \approx 1/sr$.

C.4. Necessary condition for the existence of haploid and diploid populations

If $\phi_p < 0$, the population size can never be a positive value. From this point forward, therefore, we basically discuss the relative advantage of the ploidy levels by considering only the cases where $\phi_h^{max} > 0$ and $\phi_d^{max} > 0$.

$$m_0h_h\delta(\gamma)/v_h^{\gamma}e_h < 1, \quad \text{(C.5a)}$$

$$m_0h_h\delta(\gamma)(2^{-\alpha\gamma}/r)/v_h^{\gamma}e_h < s. \quad \text{(C.5b)}$$

In the case where the conditions $\phi_h^{max} > 0$ and $\phi_d^{max} < 0$ are satisfied when we consider the extremely small s in the Figs. 2 and 3, we classified these parameter sets as the region (i), where haploids are always advent over the diploids.

C.5. Relative value of the first and second terms in Eqs. (13) and (14)

Our analytical results suggest that the boundaries between parameter regions favoring different ploidy levels are determined by the inequality between the conversion efficiency levels of diploids and haploids s, and by an expression that consists of two terms. The first term is $2^{\alpha(1-\beta-\gamma)}$ or $1/r$. The second term is proportional to $m_0h_h\delta(\gamma)/v_h^{\gamma}e_0$. Here, we show that the value of the first term is larger than the absolute value of the second term with the basic parameter set ($\alpha = 1$, $\beta = 2/3$, $r = 1$, and $0 \le \gamma \le 1$). To consider the case when the second term is very large, we set $m_0h_h\delta(\gamma)/v_h^{\gamma}e_h = 1$, from Eq. (C.5a). Then, the first and second terms of Eq. (13) are $2^{\frac{1}{3}-\gamma}$ and $2^{-\gamma}\left(1 - 2^{1/3}\right)$, and those of Eq. (14) are 1 and $1 - 2^{-\gamma}$. The value of the first term under each condition is larger than the absolute value of the second term for $0 \le \gamma \le 1$.

C.6. Patterns of the relative advantage for different values of nutrient density N

In our system, we can predict that there are five possible patterns: (i) haploidy is always advantageous over diploidy; (ii) haploidy is advantageous over diploidy under nutrient-poor conditions, and vice versa; (iii) diploidy is advantageous over haploidy under nutrient-poor conditions, and vice versa; (iv) diploidy is always advantageous over haploidy; and (v) diploidy is advantageous under both nutrient-poor and nutrient-rich conditions, and haploidy is advantageous over diploidy at intermediate nutrient densities (Figs. 2 and 3). Here, conditions (i)–(iii) can be defined by the analytical conditions, but we cannot distinguish analytically between (iv) and (v). We derive the necessary and sufficient conditions for (i)–(iii), and the necessary conditions for (iv) and (v).

For condition (i), $N_h^* < N_d^*$ and $\phi_h^{max} > \phi_d^{max}$ should be satisfied. From these, we can derive necessary and sufficient conditions for s when $s < 2^{\alpha(1-\beta-\gamma)} + \Delta_P$ when $2^{\alpha(1-\beta-\gamma)} + \Delta_P < (1/r) + \Delta_R$, or $s < (1/r) + \Delta_R$ when $2^{\alpha(1-\beta-\gamma)} + \Delta_P > (1/r) + \Delta_R$.

For condition (ii), $N_h^* < N_d^*$ and $\phi_d^{max} > \phi_h^{max}$ should be satisfied. From these, we can derive the condition $(1/r) + \Delta_R < s < 2^{\alpha(1-\beta-\gamma)} + \Delta_P$ when $2^{\alpha(1-\beta-\gamma)} + \Delta_P > (1/r) + \Delta_R$.

For condition (iii), $N_d^* < N_h^*$ and $\phi_h^{max} > \phi_d^{max}$ should be satisfied. From these, we can derive the condition $2^{\alpha(1-\beta-\gamma)} + \Delta_P < s < (1/r) + \Delta_R$ when $2^{\alpha(1-\beta-\gamma)} + \Delta_P < (1/r) + \Delta_R$.

For condition (iv) or (v), $N_d^* < N_h^*$ and $\phi_d^{max} > \phi_h^{max}$ should be satisfied. From these, we can drive the conditions $s > 2^{\alpha(1-\beta-\gamma)} + \Delta_P$ when $2^{\alpha(1-\beta-\gamma)} + \Delta_P > (1/r) + \Delta_R$, or $s > (1/r) + \Delta_R$ when $2^{\alpha(1-\beta-\gamma)} + \Delta_P < (1/r) + \Delta_R$.

C.7. Approximating the boundary between conditions (iv) and (v)

We cannot distinguish conditions (iv) and (v) analytically. These two conditions can be discriminated by the solutions of $\phi_d - \phi_h = 0$. Because this equation can be simplified as a quadratic equation and because $\phi_d > \phi_h$ when $N = 0$ and $\gamma > 0$, we can discriminate condition (v) from (iv) by examining the two characteristic roots of the equation. When both real roots are positive and these are larger than N_h^*, the region belongs to condition (v). To calculate the boundary between conditions (iv) and (v), and thus distinguish between them, we calculated the roots of the solution $\phi_d - \phi_h = 0$ by using the NSolve function of *Wolfram Mathematica* (version 10.1) and boundaries are traced using *Adobe Illustrator* manually. If the condition for the existence of a positive real root can be approximated by Eqs. (C.1a) and (C.1b), then the boundary between conditions (iv) and (v) can be approximated by Eq. (C.2). The degree of accuracy of the approximation can be checked by examining Fig. 2, which shows that the approximation tends to be valid when the strength of the non-linearity term is very small ($m_0h_h\delta(\gamma)/v_h^{\gamma}e_h \approx 0$).

Appendix D. Relative advantage of ploidy under density dependence

We examine the relative advantages of haploid and diploid populations given the population dynamics described by Eqs. (9a) and (9b), (10a) and (10b), and (11). In this system, there are four possible density for the haploid density $\overline{H}$ and of diploid density $\overline{D}$ at equilibrium: (1) Both haploids and diploids become extinct ($\overline{H}=0$ and $\overline{D}=0$); (2) haploids reach their carrying capacity and diploids become extinct ($\overline{H}=0$ and $\overline{D}=0$); (3) diploids reach their carrying capacity and haploids become extinct ($\overline{H}=0$ and $\overline{D}=0$); and (4) haploids and diploids coexist ($\overline{H}=0$ and $\overline{D}=0$). Here, we analyze each of these equilibria.

(1) Both haploids and diploids become extinct ($\overline{H}=0$ and $\overline{D}=0$)
In this case, we can calculate the equilibrium density of nutrients as $\tilde{N}=N_0 f_{in}/f_{decay}$. We find that this equilibrium point is unstable when $\phi_h(\overline{N}_0)>0$ or $\phi_d(\overline{N}_0)>0$ for $\overline{N}_0 := N_0 f_{in}/f_{decay}$. Conversely, it is stable when $\phi_h(\overline{N}_0)<0$ and $\phi_d(\overline{N}_0)<0$. These boundaries are denoted as $\overline{N}_0 = m_0 C_4/(1-m_0 h_h C_5)$ and $\overline{N}_0 = m_0 C_4 2^{\alpha(1-\beta-\gamma)}/\{s-m_0 h_h C_5 (2^{-\alpha\gamma}/r)\}$. To discuss the relative advantage of diploidy over haploidy, we consider only the case where $\phi_h(\overline{N}_0)>0$ or $\phi_d(\overline{N}_0)>0$.

(2) Haploids reach their carrying capacity and diploids become extinct ($\overline{H}=0$ and $\overline{D}=0$)
This equilibrium is stable when $\phi_h(\tilde{N})=0$ and $\phi_d(\tilde{N})<0$, and unstable when $\phi_h(\tilde{N})=0$ and $\phi_d(\tilde{N})>0$. From the equilibrium condition for the haploid density $\phi_h(\tilde{N})=0$, we have

$$\tilde{N}(\overline{H},\overline{D})=\frac{m_0 C_4}{1-m_0 h_h C_5}=N_h^*. \tag{D.1}$$

Substituting Eq. (D.1) into Eq. (11), we obtain the boundary between $\phi_d(\tilde{N})<0$ and $\phi_d(\tilde{N})>0$ as $s=2^{\alpha(1-\beta-\gamma)}+\Delta_P$. At equilibrium, the density of haploids will converge to

$$\overline{H}=\frac{N_0 f_{in}-N_h^* f_{decay}}{\tilde{U}_h(N_h^*)}. \tag{D.2}$$

(3) Diploids reach their carrying capacity and haploids become extinct ($\overline{H}=0$ and $\overline{D}=0$)
This equilibrium is stable when $\phi_h(\tilde{N})<0$ and $\phi_d(\tilde{N})=0$, and unstable when $\phi_h(\tilde{N})>0$ and $\phi_d(\tilde{N})=0$. By performing similar calculations performed for (2), we obtain the same boundary of invasibility for rare haploids $s=2^{\alpha(1-\beta-\gamma)}+\Delta_P$. At equilibrium, the density of diploids converges to

$$\overline{D}=\frac{N_0 f_{in}-N_d^* f_{decay}}{\tilde{U}_d(N_d^*)}. \tag{D.3}$$

(4) Haploids and diploids coexist ($\overline{H}=0$ and $\overline{D}=0$)

As we calculated for (2) and (3), the nutrient density at equilibrium must satisfy $\tilde{N}(\overline{H},\overline{D})=N_h^*$ for haploids and $\tilde{N}(\overline{H},\overline{D})=N_d^*$ for diploids. Only when $N_d^*=N_h^*$ do both diploids and haploids coexist along a knife edge $s=2^{\alpha(1-\beta-\gamma)}+\Delta_P$. Because the parameter values for this knife edge are a special case, we do not consider it biologically plausible. Hence, this system has no stable equilibrium point at which both H and D are strictly positive. Also, there are no periodic orbits because there is no unstable equilibrium within the first quadrant.

From the calculations in this appendix, we can conclude that our system has only two possible outcomes with regard to the equilibrium abundance of competing haploids and diploids: haploids reach their carrying capacity and diploids become extinct ($\overline{H}=0$ and $\overline{D}=0$), or diploids reach their carrying capacity and haploids become extinct ($\overline{H}=0$ and $\overline{D}=0$). The actual outcome depends on the boundary condition Eq. (13), and this condition conforms to the result obtained by a formal local stability analysis with a Jacobian matrix for the dynamics.

Appendix E. Chemostat model

In the chemostat model, the mortality rate is assumed to be approximately zero relative to the flux. Substituting $m_0\approx 0$ into Eqs. (A.4) and (A.5), we derive the intrinsic rate of population growth to be $\phi_p=\ln 2/T_p$. Substituting this into Eqs. (12a) and (12b), the population dynamics can be denoted as,

$$\frac{dH}{dt}=\left(\frac{\ln 2}{T_h}-f_{out}\right)H, \tag{E.1a}$$

$$\frac{dD}{dt}=\left(\frac{\ln 2}{T_d}-f_{out}\right)D. \tag{E.1b}$$

This system is obtained by substituting $\gamma=0$ and $m_0=f_{out}$ into Eqs. (10a) and (10b). Substituting $\gamma=0$ and $m_0=f_{out}$ into the Eqs. (C.5a) and (C.5b), we derive the following boundaries for $\phi_p^{max}>0$:

$$f_{out}h_h/e_h<1, \tag{E.2a}$$

$$f_{out}h_h(1/r)/e_h<s. \tag{E.2b}$$

By substituting $\gamma=0$ and $m_0=f_{out}$ into Eqs. (13) and (14), we can also derive the boundaries for the relative advantage of the ploidy levels for poor and rich nutrient levels:

$$s=2^{\alpha(1-\beta)}+f_{out}h_h\left\{(1/r)-2^{\alpha(1-\beta)}\right\}/e_0, \tag{E.3a}$$

$$s=1/r. \tag{E.3b}$$

Here, we note that the four boundary conditions Eqs. (E.2a), (E.2b), (E.3a), and (E.3b) intersect at one point on the ($f_{out}h_h/e_h$, s) plane: $(1, 1/r)$.

Appendix F. Parameter estimation

The parameters of the model were estimated from the results of a competition experiment performed in chemostats to measure the relative fitness of isogenic haploid and diploid strains of yeast (Adams and Hansche, 1974). We also used allometric relationships for the nutrient uptake rate reported by Edwards et al. (2012).

One premise of the nutrient-limitation hypothesis is that a positive correlation exists between nuclear DNA and cell volume; thus, the volume of a diploid cell is double that of a haploid cell (Perrot, 1994). In fact, the positive exponent α is normally estimated as one ($\alpha\approx 1$; Gregory, 2001; Price et al., 1973). Adams and Hansche (1974) reported that the average volume of diploid cells is nearly double that of haploid cells under some experimental conditions. However, some studies have reported other values (Gregory, 2001). Thus, although we normally assume $\alpha=1$, we also consider that the parameter range $0.75<\alpha<1.25$ is possible. If the cell is considered a perfect sphere, its volume is $4\pi R^3/3$ and its surface area is $4\pi R^2$, where R is the radius of the sphere. Thus, the surface area is proportional to $[volume]^{2/3}$. Hence, the exponent of the surface to volume ratio β is often fixed as 2/3 (e.g., Irie et al. 2010).

The nutrient uptake rate is often assumed to be limited by the external concentration of nutrients, and the Michaelis–Menten function is commonly used to represent this limitation (Edwards

et al., 2012; Herbert et al., 1956; Monod, 1950). Edwards et al. (2012) represented the allometric relationships between the maximum nutrient uptake rate $V^P_{max}(\mu mol/cell*day)$ and the half-saturation constants for nutrient uptake $K^P(\mu mol/l)$ in the Michaelis–Menten function for phosphate and cell volume volume(μm^3) as $V^P_{max} \approx 10^{-8.7} \times volume^{0.94}$ and $K^P \approx 10^{-1.5} \times volume^{0.53}$. Adams and Hansche (1974) reported the cell volume of yeast in their experiment to be about $v_h \approx 56(\mu m^3)$. We used these results and Eq. (A.7), and assumed that the results from experiments when all essential nutrients were present in excess (Table 1 in (Adams and Hansche, 1974)) conform to our analytical results when nutrient level is very large to obtain the parameters for the parameters of nutrient uptake rate in our model h_h $\left(10^9 * h * \mu m^3/\mu mol\right)$ and $\sigma\left(1/10^9 * \mu m^{3\beta} * h\right)$: $h_h = 24 v_h / \left\{10^9 (\ln 2) V^P_{max}\right\} \approx 22.09$ and $\sigma = \left\{10^9\left(2^{1-\beta}-1\right)V^P_{max}\right\} / \left\{24(1-\beta)v_h^\beta K^P\right\} \approx 0.73$.

Adams and Hansche (1974) also reported the doubling time of yeast T(h) to be $T_h \approx 2.5$ under nutrient-rich conditions. We thus estimated the energy conversion efficiency $e_h\left(10^9 * \mu m^3/\mu mol\right)$ with equation, $e_h \approx h_h(ln2)/T_h \approx 6.13$. The experimentally determined dilution rate in a chemostat was $f_{out} = 0.17(1/h)$. This value is almost 60% of the maximum population growth rate with the estimated parameters as they reported.

We considered parameters s and r for the ploidy-dependent regulation of the gene expression level (gene dosage effect). The nutrient-limitation hypothesis assumes that twice as much DNA allows twice the transcription of mRNA in a diploid cell but that this advantage is canceled out by the double volume of the diploid cell. Therefore, the diploid cell utilization efficiency is assumed to almost the same as that of a haploid cell (Perrot, 1994). A correlation between the nuclear level of regulation (expression, repression) of an autosomal gene and the number of chromosome sets (structural gene dosage) is often observed in higher eukaryotic organisms (DeMaggio and Lambrukos, 1974; Guo et al., 1996; Suzuki et al., 1999; Timko et al., 1980). Adams and Hansche (1974) reported no significant difference in doubling time between haploid and diploid cells under nutrient-rich conditions. This result conforms to the assumption of the nutrient-limitation hypothesis because from Eq. (A.2), the relative length of a generation time is $T_h/T_d \approx sr$ under nutrient-rich condition. Hence, we normally assume $s=1$ and $r=1$.

References

Abbott, I.A., Hollenberg, G.J., 1993. Marine Algae of California. Stanford Univ Press, Stanford. Calfornia.

Adams, J., Hansche, P.E., 1974. Population studies in microorganisms I. Evolution of diploidy in *Saccharomyces cerevisiae*. Genetics 76, 327–338.

Aksnes, D., Egge, J., 1991. A theoretical model for nutrient uptake in phytoplankton. Mar. Ecol. Prog. Ser. 70, 65–72.

Bell, G., 1994. The comparative biology of the alternation of generations. Lect. Math. Life Sci. 25, 1–26.

Bell, G., 1997. The evolution of the life cycle of brown seaweeds. Biol. J. Linn. Soc. 60, 21–38.

Bennett, M., 1971. The duration of meiosis. Proc. R. Soc. Lond. Ser. B Biol. Sci. 178, 277–299.

Bennett, M., 1972. Nuclear DNA content and minimum generation time in herbaceous plants. Proc. R. Soc. Lond. Ser. B. Biol. Sci. 181, 109–135.

Bessho, K., Iwasa, Y., 2010. Optimal seasonal schedules and the relative dominance of heteromorphic and isomorphic life cycles in macroalgae. J. Theor. biol. 267, 201–212.

Cavalier-Smith, T., 1978. Nuclear volume control by nucleoskeletal DNA, selection for cell volume and cell growth rate, and the solution of the DNA C-value paradox. J. Cell Sci. 34, 247–278.

Coelho, S.M., Peters, A.F., Charrier, B., Roze, D., Destombe, C., Valero, M., Cock, J.M., 2007. Complex life cycles of multicellular eukaryotes: new approaches based on the use of model organisms. Gene 406, 152–170.

Commoner, B., 1964. Roles of deoxyribonucleic acid in inheritance. Nature 202, 960–968.

Crow, J., Kimura, M., 1965. Evolution in sexual and asexual populations. Am. Nat., 439–450.

DeMaggio, A., Lambrukos, J., 1974. Polyploidy and gene dosage effects on peroxidase activity in ferns. Biochem. Genet. 12, 429–440.

Destombe, C., Godin, J., Nocher, M., Richerd, S., Valero, M., 1993. Differences in response between haploid and diploid isomorphic phases of *Gracilaria verrucosa* (Rhodophyta: Gigartinales) exposed to artificial environmental conditions. Hydrobiologia 260, 131–137.

Dring, M.J., 1992. The biology of marine plants. Cambridge Univ Press, New York.

Edwards, K.F., Thomas, M.K., Klausmeier, C.A., Litchman, E., 2012. Allometric scaling and taxonomic variation in nutrient utilization traits and maximum growth rate of phytoplankton. Limnol. Oceanogr. 57, 554–566.

Francis, J.C., Hansche, P.E., 1972. Directed evolution of metabolic pathways in microbial populations I. Modification of the acid phosphatase pH optimum in *S. cerevisiae*. Genetics 70, 59–73.

Galitski, T., Saldanha, A.J., Styles, C.A., Lander, E.S., Fink, G.R., 1999. Ploidy regulation of gene expression. Science 285, 251–254.

Gentleman, W., Leising, A., Frost, B., Strom, S., Murray, J., 2003. Functional responses for zooplankton feeding on multiple resources: a review of assumptions and biological dynamics. Deep Sea Res. Part II: Top. Stud. Oceanogr. 50, 2847–2875.

Gerstein, A.C., Otto, S.P., 2009. Ploidy and the causes of genomic evolution. J. Hered. 100, 571–581.

Gerstein, A.C., McBride, R.M., Otto, S.P., 2008. Ploidy reduction in *Saccharomyces cerevisiae*. Biol. Lett. 4, 91–94.

Gerstein, A.C., Chun, H.-J.E., Grant, A., Otto, S.P., 2006. Genomic convergence toward diploidy in *Saccharomyces cerevisiae*. PLoS Genet. 2, e145.

Glazunov, A., Boreĭko, A., Esser, A., 1989. Relative competitiveness of haploid and diploid yeast cells growing in a mixed population. Mikrobiologiia 58, 769–777 (in Russian, abstract in English).

Goff, L.J., Coleman, A.W., 1990. Chapter 3 DNA: microspectrofluorometric studies. In: Cole, K.M., Sheath, R.G. (Eds.), Cambridge University Press, New York, pp. 43–71.

Gregory, T., 2001. Coincidence, coevolution, or causation? DNA content, cellsize, and the C-value enigma. Biol. Rev. 76, 65–101.

Guo, M., Davis, D., Birchler, J.A., 1996. Dosage effects on gene expression in a maize ploidy series. Genetics 142, 1349–1355.

Herbert, D., Elsworth, R., Telling, R., 1956. The continuous culture of bacteria; a theoretical and experimental study. J. Gen. Microbiol. 14, 601–622.

Holling, C.S., 1959. Some characteristics of simple types of predation and parasitism. Can. Entomol. 91, 385–398.

Holm-Hansen, O., 1969. Algae: amounts of DNA and organic carbon in single cells. Science 163, 87–88.

Hori, T., 1994. An Illustrated atlas of the life history of algae: 1. Green algae; 2. Brown and red algae; 3. Unicellular and flagellated algae. Uchida Rkakuho, Tokyo (Japanese).

Hughes, J.S., Otto, S.P., 1999. Ecology and the evolution of biphasic life cyclesAm. Nat. 154, 306–320.

Irie, T., Bessho, K., Findlay, H.S., Calosi, P., 2010. Increasing costs due to ocean acidification drives phytoplankton to be more heavily calcified: optimal growth strategy of coccolithophores. PloS One 5, e13436.

Jenkins, C.D., 1993. Selection and the evolution of genetic life cycles. Genetics 133, 401–410.

Jovtchev, G., Schubert, V., Meister, A., Barow, M., Schubert, I., 2006. Nuclear DNA content and nuclear and cell volume are positively correlated in angiosperms. Cytogenet. Genome Res. 114, 77–82.

Kondrashov, A.S., Crow, J.F., 1991. Haploidy or diploidy: which is better? Nature 351, 314–315.

Lewis, J., Wolpert, L., 1979. Diploidy, evolution and sex. J. Theor. Biol. 78, 425–438.

Lewis Jr., W.M., 1985. Nutrient scarcity as an evolutionary cause of haploidy. Am. Nat. 125, 692–701.

Littler, M.M., Littler, D.S., Taylor, P.R., 1987. Functional similarity among isomorphic life-history phases of *Polycavernosa debilis* (Rhodophyta, Gracilariaceae). J. Phycol. 23, 501–508.

M'Gonigle, L.K., Otto, S.P., 2011. Ploidy and the evolution of parasitism. Proc. R. Soc. B: Biol. Sci. 278, 2814–2822.

Mable, B.K., Otto, S.P., 2001. Masking and purging mutations following EMS treatment in haploid, diploid and tetraploid yeast (*Saccharomyces cerevisiae*). Genet. Res. 77, 9–26.

Mable, K.B., Otto, P.S., 1998. The evolution of life cycles with haploid and diploid phases. BioEssays 20, 453–462.

Martin, P., 1966. Variation in the amounts of nucleic acids in the cells of different species of higher plants. Exp. Cell Res. 44, 84–94.

Melaragno, J.E., Mehrotra, B., Coleman, A.W., 1993. Relationship between endopolyploidy and cell size in epidermal tissue of Arabidopsis. Plant Cell Online 5, 1661–1668.

Michod, R.E., Gayley, T., 1994. Genetic error, heterozygosity and the evolution of the sexual life cycle. Lect. Math. Life Sci. 25, 97–120.

Monod, J., 1950. La technique de culture continue: Théorie et applications. Ann. Inst. Pasteur 79, 390–410.

Naïdhardt, K., Glazunov, A., 1991. Competition of isogenic haploid and diploid cells of *Saccharomyces cerevisiae* and *Pichia pinus* growing in a mixed population. (in Russian, Abstract in English). Mikrobiologiia 60, 686–692.

Nuismer, S.L., Otto, S.P., 2004. Host-parasite interactions and the evolution of ploidy. Proc. Natl. Acad. Sci. USA 101, 11036–11039.

Olmo, E., Morescalchi, A., 1978. Genome and cell sizes in frogs: a comparison with salamanders. Cell. Mol. Life Sci. 34, 44–46.

Orr, H.A., Otto, P.S., 1994. Does diploidy increase the rate of adaptation? Genetics 136, 1475–1480.
Otto, S., Goldstein, D., 1992. Recombination and the evolution of diploidy. Genetics 131, 745–751.
Otto, S.P., Marks, J.C., 1996. Mating systems and the evolutionary transition between haploidy and diploidy. Biol. J. Linn. Soc. 57, 197–218.
Otto, S.P., Gerstein, A.C., 2008. The evolution of haploidy and diploidy. Curr. Biol. 18, R1121–R1124.
Pagel, M., Johnstone, R.A., 1992. Variation across species in the size of the nuclear genome supports the junk-DNA explanation for the C-value paradox. Proc. R. Soc. Lond. Ser. B: Biol. Sci. 249, 119–124.
Paquin, C., Adams, J., 1983. Frequency of fixation of adaptive mutations is higher in evolving diploid than haploid yeast populations. Nature 302, 495–500.
Perrot, V., 1994. Experimental approaches to the evolution of life cycles. Lect. Math. Life Sci. 25, 121–134.
Perrot, V., Richerd, S., Valéro, M., 1991. Transition from haploidy to diploidy. Nature 351, 315–317.
Price, H.J., Sparrow, A.H., Nauman, A.F., 1973. Correlations between nuclear volume, cell volume and DNA content in meristematic cells of herbaceous angiosperms. Cell. Mol. Life Sci. 29, 1028–1029.
Real, L.A., 1977. The kinetics of functional response. Am. Nat. 111, 289–300.
Solomon, M.E., 1949. The natural control of animal populations. J. Anim. Ecol., 1–35.
Suzuki, M.G., Shimada, T., Yokoyama, T., Kobayashi, M., 1999. The influence of triploidy on gene expression in the silkworm, *Bombyx mori*. Heredity 82, 661–667.
Timko, M.P., Vasconcelos, A.C., Fairbrothers, D.E., 1980. Euploidy in Ricinus. I. Euploidy and gene dosage effects on cellular proteins. Biochem. Genet. 18, 171–183.
Van den Hoek, C., Mann, D., Jahns, H., 1995. Algae: an introduction to phycology. Cambridge University Press.
Van't Hof, J., 1965. Relationships between mitotic cycle duration, S period duration and the average rate of DNA synthesis in the root meristem cells of several plants. Exp. Cell Res. 39, 48–58.
Van't Hof, J., Sparrow, A.H., 1963. A relationship between DNA content, nuclear volume, and minimum mitotic cycle time. Proc. Natl. Acad. Sci. USA 49, 897–902.
Weiss, R.L., Kukora, J., Adams, J., 1975. The relationship between enzyme activity, cell geometry, and fitness in *Saccharomyces cerevisiae*. Proc. Natl. Acad. Sci. USA 72, 794–798.
Ycas, M., Sugita, M., Bensam, A., 1965. A model of cell size regulation. J. Theor. Biol. 9, 444–470.